Original Article

Minute pulmonary meningothelial-like nodules: associations between computed tomography and pathology features

Yawen Zhang[1,2#], Jing Wu[1#], Youcai Zhao[3], Tao Zhang[1], Hai Xu[4], Yu-Chen Chen[1]

[1]Department of Radiology, Nanjing First Hospital, Nanjing Medical University, Nanjing, China; [2]Department of Radiology, Nanjing Pukou District Central Hospital, Nanjing, China; [3]Department of Pathology, Nanjing First Hospital, Nanjing Medical University, Nanjing, China; [4]Department of Radiology, the First Affiliated Hospital of Nanjing Medical University, Nanjing, China

Contributions: (I) Conception and design: Y Zhang; (II) Administrative support: YC Chen; (III) Provision of study materials or patients: H Xu; (IV) Collection and assembly of data: J Wu; (V) Data analysis and interpretation: Y Zhao, T Zhang; (VI) Manuscript writing: All authors; (VII) Final approval of manuscript: All authors.

[#]These two authors contributed equally to this work.

Correspondence to: Yu-Chen Chen. Department of Radiology, Nanjing First Hospital, Nanjing Medical University, 68 Changle Road, Nanjing 210006, China. Email: chenyuchen1989@126.com; Hai Xu. Department of Radiology, the First Affiliated Hospital of Nanjing Medical University, 300 Guangzhou Road, Nanjing 210029, China. Email: 13913870103@126.com.

Background: Increased use of multislice computed tomography (CT) scans has revealed that minute pulmonary meningothelial-like nodules (MPMNs) showed as ground-glass nodules (GGNs) are frequent in patients. However, little is known about the incidence and fate of nodules. By using a cross-sectional design, this study compared the multislice CT signs and pathological results of MPMNs, and further used pathological results to explain the formation mechanism of the CT signs of MPMNs to improve the clinical understanding of the disease.

Methods: The clinicopathological data of 93 cases diagnosed as MPMNs in the Jiangsu Province Hospital from January 2016 to September 2019 and the Nanjing First Hospital from January 2017 to December 2019 were examined. The related literature was reviewed, and each case's age, gender, medical history, and preoperative CT examinations were classified. Based on CT signs, this study analyzed the imaging features, including size, shape, boundary, distribution, opacity, and their relationship with pulmonary blood vessels.

Results: A total of 13 cases had immunohistochemistry results among which the lesions showed consistent positive expression of vimentin (100%), followed by epithelial cell membrane antigen (92.3%) and progesterone (8%). The MPMNs mainly occurred in individuals aged 50–59 years (32.6%). Most patients (82.6%) had neoplastic disease. All nodules (100%) manifested with a round shape and well-demarcated borders on images. The size of the nodules on CT scans ranged from 2.5 to 5.0 mm, with an average size of 3.04±1.12 mm. Most nodules were subpleural (89.1%) and showed ground-glass opacity (97.8%). The follow-up results of postoperative clinical manifestations and chest CT examination were negative in 12 patients.

Conclusions: This study suggested that the pathological findings of MPMNs could explain the formation mechanism of the CT signs. The results can provide guidance for the diagnosis of the disease in the future.

Keywords: Minute pulmonary meningothelial-like nodules (MPMNs); ground-glass nodules (GGNs); computed tomography (CT); pathology

Submitted Dec 31, 2021. Accepted for publication Aug 29, 2022. Published online Oct 08, 2022.
doi: 10.21037/qims-21-1250
View this article at: https://dx.doi.org/10.21037/qims-21-1250

Introduction

Minute pulmonary meningothelial-like nodules (MPMNs) are often incidentally detected in surgical or autopsy specimens of the lung during routine pathological examinations (1,2). In recent years, the development of medical equipment and the widespread use of computed tomography (CT) have increased the detection rate of MPMNs. Our literature search yielded few articles involving imaging studies, and there was a particular lack of imaging and pathological correlation analysis. The sample sizes in existing studies were relatively small, and previous articles did not follow up with the patients after surgery.

The pathogenesis of MPMNs is currently unclear. Although MPMNs are usually small, parts of MPMNs can be detected by CT as single or multiple ground-glass nodules (GGNs) (3,4). Due to the lack of specific characteristics, it is difficult to distinguish MPMNs from atypical adenomatous hyperplasia (AAH), adenocarcinoma in situ (AIS), and minimally invasive adenocarcinoma (MIA). It is also difficult to distinguish multiple lesions from metastatic tumors.

The objective of our study was to compare the CT signs and pathological features of MPMNs and further use these features to explain the formation mechanism of CT signs to provide therapeutic insight for clinical practice. We present the following article in accordance with the STROBE reporting checklist (available at https://qims.amegroups.com/article/view/10.21037/qims-21-1250/rc).

Methods

Study population

This study used a cross-sectional study design. We used two separate datasets from two centers: 12,000 lung resection specimens from the Department of Pathology at the Jiangsu Province Hospital from January 2016 to September 2019, further screening 88 cases of pulmonary micromeningioma-like nodules, and 1,500 lung resection specimens from the Department of Pathology at the Nanjing First Hospital from January 2017 to December 2019, screening another 5 cases of pulmonary micromeningioma-like nodules. The data of a total of 93 patients were collected from the two hospitals, each with detailed individual clinical cases, including chest images before surgery and postoperative pathology results. The study was conducted in accordance with the Declaration of Helsinki (as revised in 2013). The current study was approved by the Institutional Review Board of Nanjing Medical University. All participants provided informed consent for article publications and the use of any accompanying images. The flow diagram of this study is shown in *Figure 1*.

CT examination

Chest CT examinations were conducted with a 64/128 channel Siemens CT (Siemens Medical Solutions, Erlangen, Germany) or 64/128 Philips CT (Ingenuity; Philips, Eindhoven, Netherlands). The scanner protocol was 120 kV peak and 100 effective mAs with dose modulation.

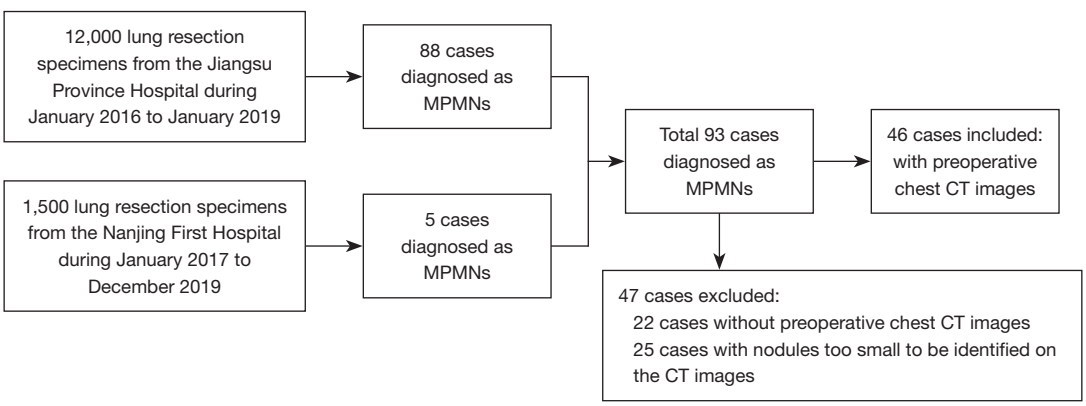

Figure 1 The flow diagram of this study. MPMNs, minute pulmonary meningothelial-like nodules; CT, computed tomography.

Reconstruction intervals were 5 mm thick at 5 mm intervals without gaps and 1.5 mm thick without gaps. Both hospitals performed standardized scans on patients. A supine position was used for scanning, and patients were spiral scanned from the entrance of the chest to 2 cm below the diaphragm. The following scanning and image post-processing parameters were used: collimator width, 1.2 mm; pitch value, 0.9; the lung window was reconstructed with a 5 and 1.5 mm layer thickness bone algorithm; and the mediastinal window was reconstructed with a 5 mm layer thickness soft tissue algorithm [lung window width, 1,200 Hounsfield units (HU); window level, 600 HU; width of the mediastinal window, 350 HU; window level, 50 HU].

Clinical and radiological evaluation

Pathological specimens of MPMNs were collected from two different scenarios. Some MPMNs were confirmed by pathology after surgical resection due to misdiagnosis, and the other MPMNs were found incidentally in the background alveolated lung parenchyma. In the first condition, MPMNs could be seen and located on a chest CT scan, and in the second condition, a radiologist and pathologist determined the specific position of a lesion on the CT images according to its size and location. This process detected a further 46 MPMN patients. If the specific location of the lesions could not be observed on the CT images, it was considered that they could only be observed with a microscope.

For all pathologically confirmed cases, we identified their age, gender, and clinical and risk factors using the mean age and percentage statistics for other quantitative data. For cases with positive images, we analyzed the size, number, and distribution of the nodules. Analysis of these data used quantitative methods and percentage statistics. For cases with lesions that could not be found on CT due to their small size, the lesions were considered to be visible only under the microscope.

Pathology analysis

The surgical specimens were fixed in 4% neutral formaldehyde, embedded in paraffin, and stained with hematoxylin and eosin. The lesion histological features were observed with an optical microscope. Immunohistochemical (IHC) staining was performed using the EnVision two-step method and 3,3N-diaminobenzidine tertrahydrochloride (DAB) color development. The following antibodies were used: epithelial membrane antigen (EMA), S-100 protein, vimentin, progesterone receptor (PR), CK7, thyroid transcription factor (TTF-1), napsin A, synaptophysin (Syn), CgA, CD56, and Ki-67. All reagents were purchased from Fuzhou MaiXin Company (Fuzhou, China), and antibody staining was performed according to the manufacturer's instructions.

Results

The 93 patients included 73 females (78.5%) and 20 males (21.5%) with a mean age of 57.2 years (range, 30 to 80 years). It was found that MPMNs mainly occurred in individuals aged 60–69 years (36.6%). The detection rates of surgical lung specimens in the Jiangsu Province Hospital and Nanjing First Hospital were 0.73% and 0.33%, respectively. A total of 78 patients (83.9%) had neoplastic disease, of which there were 19 cases of AAH and AIS, one case of squamous cell carcinoma, 55 cases of adenocarcinoma, and one case each of esophageal cancer, metastatic fibrosarcoma, and hamartoma. A total of 9 patients (9.7%) had pulmonary inflammation. The pathological results showed that the inflammation was a fibrous proliferation of chronic inflammatory tissue. One patient (1.1%) had tuberculosis, and five patients (5.4%) had no tumor or inflammatory lesions. All patients were diagnosed by surgery and pathology.

According to pathological results, 93 cases of MPMNs appeared as solitary nodules in 45 cases and multiple nodules in 48 cases. The size of the nodules ranged from 1.0 to 5.0 mm. Nodules manifested with a round shape and well-demarcated borders (100%). We observed nodules close to pulmonary blood vessels.

At low magnification, lung biopsy revealed that the alveolar wall thickened to form multiple small, clear, meningeal epithelioid nodules. At high magnification, the lesions appeared as round, oval, or spindle-shaped cell nests in the lung interstitium with clear cell membranes. Lesions had rich cytoplasm, weak eosinophilia, and fine granular chromatin. Nuclei were elliptical without obvious nuclear atypia, and some cells had very small nucleoli without obvious mitotic patterns. After reviewing the original data and supplementary tests, 13 cases had IHC results, but the rest of the lesional cells were small and disappeared after immunolabeling sections. The lesional cells showed consistent positive expression of vimentin (100%), followed by epithelial cell membrane antigen (92.3%) and PR (8%).

Since we screened 46 cases based on the images, we

Table 1 Demographic and clinical characteristics of MPMNs patients (n=46)

Clinical features	Number (%)
Gender	
Female	39 (84.8)
Male	7 (15.2)
Age (years), median (range)	57.8 (38–79)
30–39	1 (2.2)
40–49	10 (21.7)
50–59	15 (32.6)
60–69	11 (23.9)
70–79	9 (19.6)
Accompanying diseases	
Neoplastic disease	38 (82.6)
Pulmonary inflammation	5 (10.9)
Tuberculosis	1 (2.2)
Asymptomatic physical examination	2 (4.3)

MPMNs, minute pulmonary meningothelial-like nodules.

further analyzed and contrasted their clinical and imaging characteristics. The clinical data for the patients are summarized in *Table 1*. Further, 46 cases were detectable by CT imaging. All nodules (100%) manifested with a round shape and well-demarcated borders, and the size of the nodules on CT scans ranged from 2.5 to 5.0 mm, with an average size of 3.04±1.12 mm. Nodules in 14 patients (30.4%) appeared as solitary nodules (*Figure 2*), and multiple nodules were present in 32 patients (69.6%) (*Figure 3*). We divided the nodules into two categories according to their distribution: nodules with a distance from the visceral pleura less than 1 cm were defined as subpleural, and those with a distance greater than 1 cm were defined as intrapulmonary. The distribution of nodules tended to be subpleural in 41 patients (89.1%) and intrapulmonary in 5 patients (10.9%). Nodules showed ground-glass opacity (GGO) in 45 patients (97.8%); among them, one patient showed diffuse GGNs in the bilateral lungs with cyst-like morphology (*Figure 4*), and one patient showed GGO with calcification (2.2%). The edges of some nodules were close to pulmonary blood vessels in 25 patients (54.3%) (*Figure 5*). We conducted clinical follow-up and chest CT reexamination of postoperative patients. Images of the chest showed that eight patients had no change in six months, three patients had no change in one year, and one patient had no change as shown by the chest CT examination for 3 years after surgery (*Figure 6*). All patients had no relevant uncomfortable symptoms. The individual image features for each patient are presented in *Table 2*.

Comparison of the size, shape, edge, opacity, and vascular relationship of individual details from CT imaging results showed good concordance with the pathology results. Therefore, pathology results could explain the appearance of different features observed by CT imaging.

Discussion

Since their first description by Korn *et al.* (5) in 1960, the exact origin and nature of MPMNs had remained undefined until now. In an IHC study, Kraushaar *et al.* (6) found that primary pulmonary meningioma appeared as a giant form of MPMN, including positive PR and CD56 staining. Later, genetic analysis of these structures indicated a reactive origin rather than a neoplastic origin (6). The new term "minute meningothelial nodule" was proposed by Gaffey *et al.* (7) and defined as "minute meningothelial nodule" in the third edition of the World Health Organization International Histological Classification of Tumors (8). When the nodules show diffusely distribution in bilateral lungs, we can diagnose them as diffuse pulmonary meningotheliomatosis (DPM) or MPMN-omatosis (9). By this definition, we further screened two cases diagnosed as diffuse pulmonary meningotheliomatosis.

Previous studies show that the detection rate of MPMN by autopsy is 0.07–4.9% (3), yet when pathologists specifically search for such lesions, the detection rate increases by more than tenfold (10). By contrast, the detection rate of surgically resected specimens is 7–13.8% (3), which is much higher than the detection rate at autopsy. Thus, we believe that the actual incidence of MPMNs is higher than that reported.

We found that MPMNs occurred in females (78.5%) more than in males, which was consistent with previous literature (3). The mechanism for this difference is currently unknown, but many studies have shown that MPMN cells are positive for progesterone expression. Progesterone stimulation may promote cell growth in lung adenocarcinoma and MPMNs, which may explain why the disease is more common in female patients than in males (3). Our data also supported the conclusions reported in the literature.

There was a higher occurrence of MPMNs in patients with malignant lung tumors (83.9%). Our results were

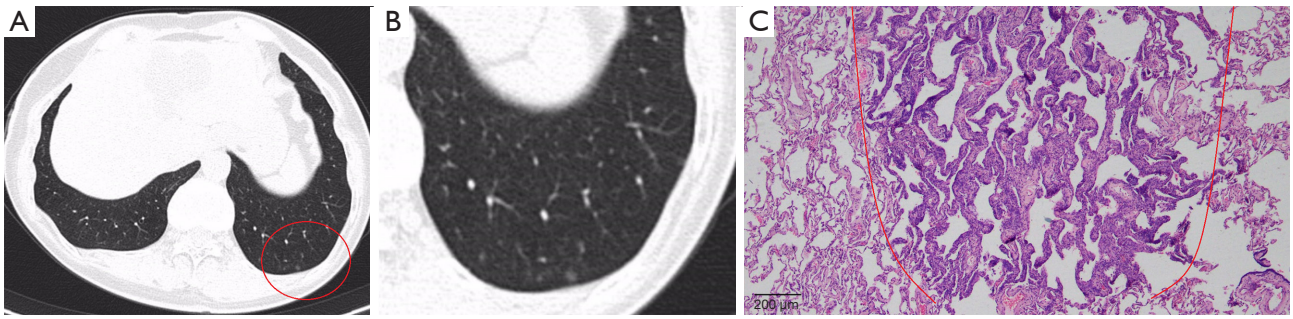

Figure 2 A 70-year-old female patient underwent a routine physical examination on May 21, 2019. (A,B) CT image of a round-shaped nodule (red circle) (CT axis). (C) The corresponding area outlines the lesion with a red line (HE, ×40; scale bar =200 μm). CT, computed tomography; HE, hematoxylin and eosin.

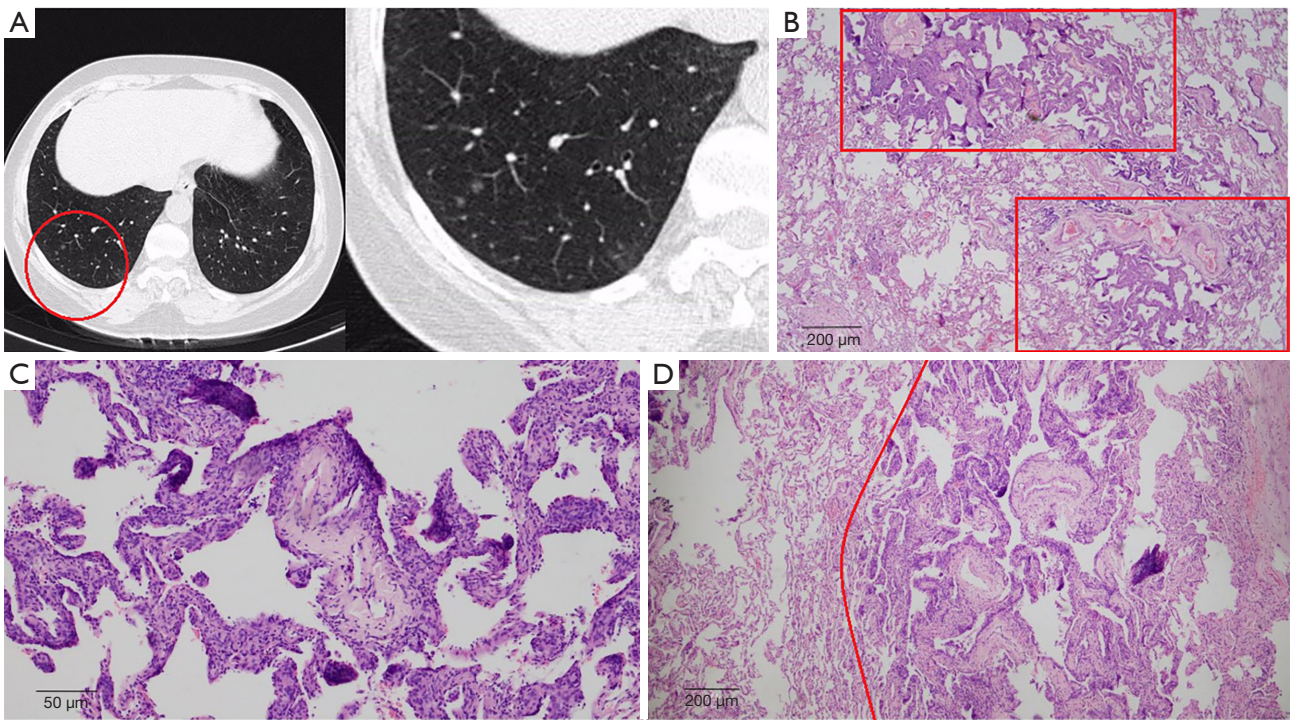

Figure 3 A 70-year-old female patient underwent a routine physical examination. (A) Two nodules in the right lower lung (red circle) (computed tomography axis). (B) The corresponding area outlines two meningioma-like nodules with red frames (HE, ×40; scale bar =200 μm). (C) Meningioma cells growing along the alveolar epithelial wall are evident, and air shadows can be seen in the alveolar space (HE, ×200; scale bar =50 μm). (D) The corresponding boundary of the nodule is clear (HE, ×40; scale bar =200 μm). HE, hematoxylin and eosin.

consistent with these previous findings which showed that patients with malignant lung tumors had a higher incidence of MPMNs than patients with other lung diseases (7.3% *vs.* 2.5%; P=0.044) (3). Particularly, lung adenocarcinoma was the most common type compared with other primary pulmonary malignant tumors [9.4% *vs.* 4.5%; odds ratio (OR) 2.33; 95% CI: 1.35; 4.02; P<0.01] (11). The microenvironment theory suggests that the external environment is the main contributing factor to the occurrence of MPMNs. Therefore, lung disease may provide a localized microenvironment that

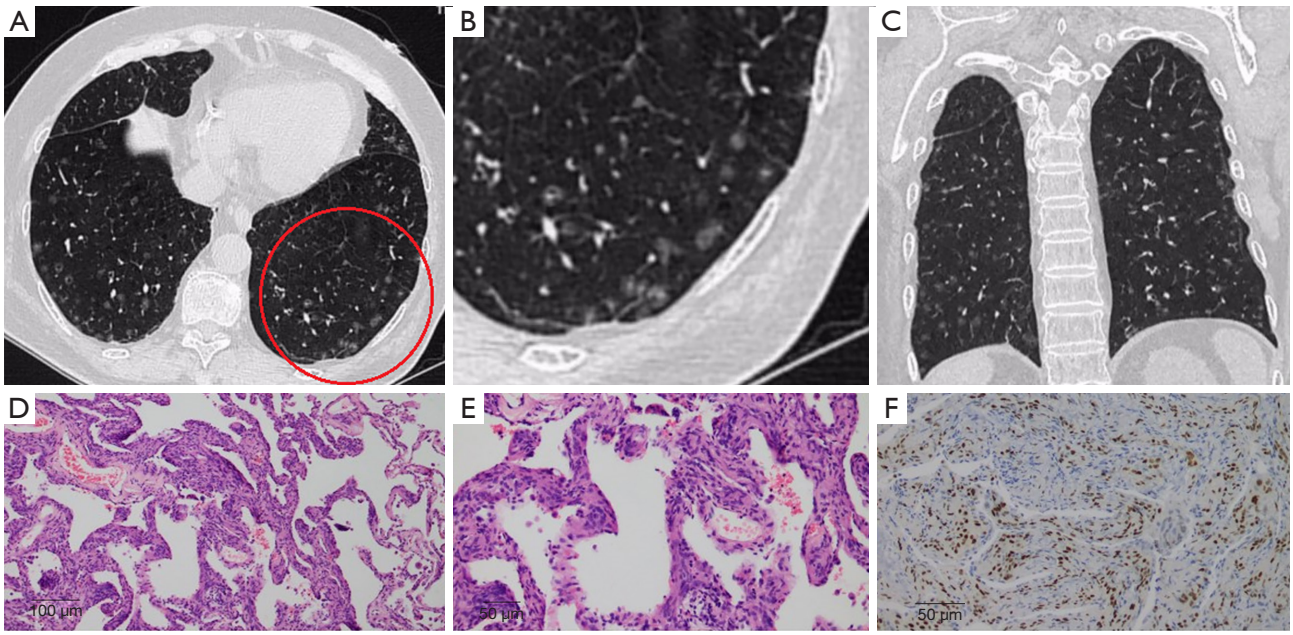

Figure 4 A 71-year-old female patient complained of a cough in December 2016. (A-C) The thin-slice CT images show diffuse ground-glass nodules in the bilateral lungs. Some of the nodules appear to have a cyst-like morphology (red circle). Nodules are randomly distributed in the lungs, measured 2–3 mm in diameter, and tend to be located in the peripheral zone (CT axis). Alveolar structure is well preserved, pulmonary septum is widened, and alveolar surface epithelial hyperplasia is not obvious in (D) (HE, ×100; scale bar =100 μm). The epithelioid cells in the high-magnification septum are uniform in size, with oval nuclei, fine chromatin, no obvious atypia and mitosis, and acidophilic cytoplasm in (E) (HE, ×200; scale bar =50 μm). (F) Immunohistochemistry of progesterone receptor showed positive nuclear staining of meningothelial-like cells (AR-200). CT, computed tomography; HE, hematoxylin and eosin.

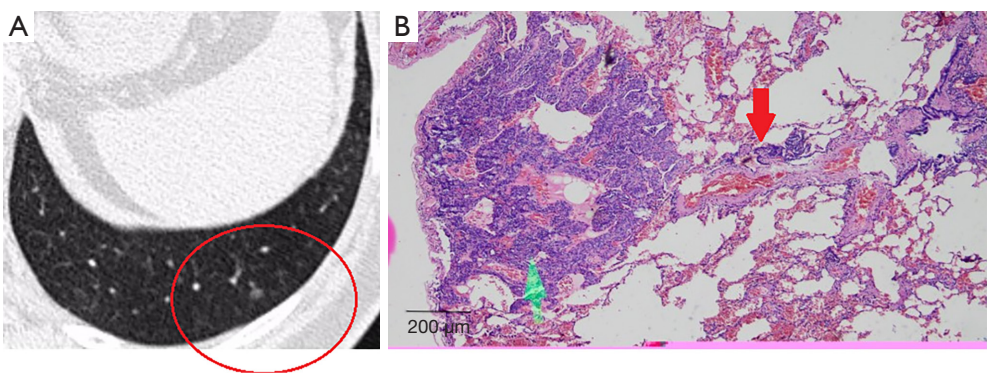

Figure 5 A 48-year-old female patient underwent a routine physical examination. (A) The thin-slice CT image shows a ground-glass nodule (red circle) under the pleura of the left lower lung, with a round shape and clear edges (CT axis). (B) Pathology shows the edge of the lesion (green arrow) is connected to the blood vessel (red arrow) (HE, ×40; scale bar =200 μm). CT, computed tomography; HE, hematoxylin and eosin.

promotes MPMN development (3).

A total of 88 cases of MPMN were confirmed due to their primary disease and five patients were diagnosed by CT examination without other diseases. These five patients were misdiagnosed with adenocarcinoma and underwent surgery. Therefore, accurate diagnosis based on imaging results is of great importance for patients and clinicians to make appropriate treatment plans.

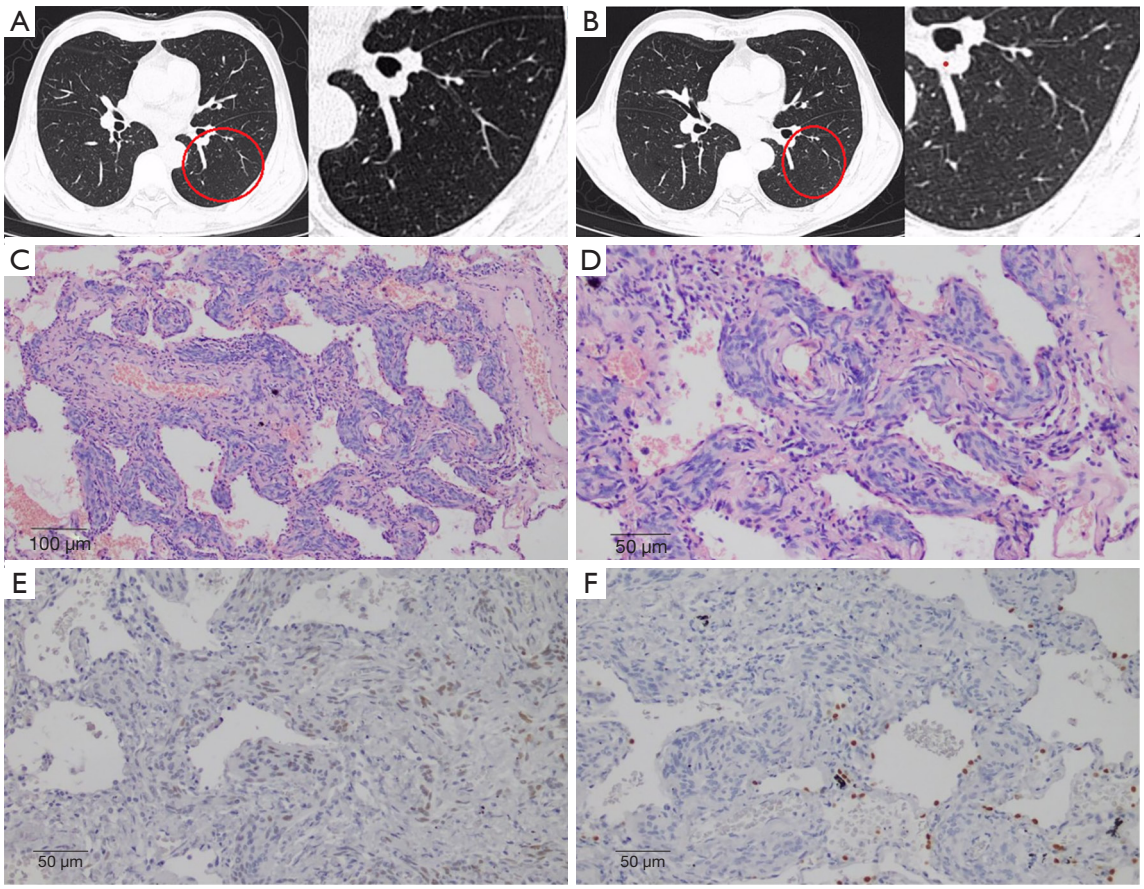

Figure 6 A 48-year-old male patient underwent a routine chest CT examination on 4 April 2018. We found a pulmonary nodule in the left lower lung. On 10 December of the same year, the patient had a chest CT scan. The nodule was similar to the previous one. (A) The thin-slice CT showed a round ground-glass nodule with clear edges in the lower left lung on April 4, 2018 (red circle) (CT axis). (B) The thin-slice CT showed a lung nodule similar to the previous one on December 10, 2018 (red circle) (CT axis). Pathological sections showed the lesion forms a well-defined nodule, located in the alveolar septa on (C) (HE, ×100; scale bar =100 μm). Pathological sections showed bland short spindle or oval cells in bundles or swirling arrangements on (D) (HE, ×200; scale bar =50 μm). The immunohistochemical staining corresponding to the (C) and (D) regions confirm that the lesions express progesterone receptor, and the alveolar epithelium expresses thyroid transcription factor in (E) TTF-1 and (F) AR-200. CT, computed tomography; HE, hematoxylin and eosin.

Nodule size on CT scans ranged from 2.5 to 5.0 mm, with an average size of 3.04±1.12 mm. Nodule size ranged from 1 to 5 mm under the microscope. The nodule size measured on CT was larger than the corresponding pathological measurement. The MPMNs appeared as round nodules on images and oval nodules under the microscope. As the alveolar space was still inflated, nodules were inevitably squeezed during surgery, resulting in the small difference in measurement results.

Lung nodules in 46 patients were all well-defined. We could observe multiple nodules in one field of sight and outline them through a low-power microscope. They appeared with clear boundaries on images. Through imaging and comparison by pathology, it can be inferred that the disease originates from the lung interstitium.

Most lesions tended to be subpleural (89.1%). Pathological examination confirmed that nodules were close to the pleura but did not involve the pleura; this result supported the conclusions reported in previous literature (3). Literature has reported that, pathologically, MPMNs are distributed along the pulmonary vessel (3). In this dataset, from the pathologic sections of 25 patients (54.3%), we could

Table 2 Descriptive results of patients' imaging characteristics (n=46)

CT features	Number (%)
Nodule number	
Single	14 (30.4)
Multiple	32 (69.6)
Opacity	
Pure ground-glass opacity	45 (97.8)
Ground-glass opacity with calcification	1 (2.2)
Shape	
Round	46 (100.0)
Edge	
Clear	46 (100.0)
Blurred	0
Distribution	
Subpleural	41 (89.1)
Intrapulmonary	5 (10.9)

CT, computed tomography.

observe the vascular course around the nodules. However, whether there was an association between the nodules and blood vessels remained unknown. According to our observation of pathology, these vessels had smooth walls and uniform lumen thickness, indicating that the growth rate of the lesion was slow and supporting the finding that the lesion was a benign nodule (12).

Most MPMNs were identified incidentally during physical examination or lung disease resection. The lesions grew inert and had a good prognosis (13). We conducted clinical follow-up and chest CT reexamination of postoperative patients. The images of the chest showed that eight patients did not have any new nodules or enlargement of the original nodules after the initial examination. Some physicians have followed up with patients at 10 and 20 years and have found that lesions are enlarged in volume but that there is no evidence of malignancy (3). Most studies have shown that MPMNs are reactive rather than of a neoplastic origin (14). Currently, MPMNs mainly require conservative observation and other related supportive therapies in clinical practice.

Most MPMNs showed GGO (97.8%). According to pathology observations, lesions originated from the alveolar interstitium rather than alveolar epithelial tissue. The lesions grew along the alveolar septum, leading to interstitial lung hyperplasia. However, the pulmonary alveoli were still inflated, so CT scans showed a GGO. Part of the nodules appeared to have a cyst-like morphology. We speculated that the pathological basis might be that the obvious pulmonary interstitial hyperplasia and contraction lead to abnormal expansion of the adjacent alveolar ducts or bronchiole, leading to a central low-opacity shadow in part of nodules (15).

There are several limitations to this study. In a retrospective analysis of CT and pathology images, when determining the specific location by CT imaging, there may be deviation even if there is a preoperative CT-guided positioning image, especially for patients with multiple MPMNs. Manual measurement errors were difficult to avoid. In addition, the sample size was limited to 46 patients that could be observed by CT imaging. Therefore, additional samples are needed in subsequent studies.

In conclusion, MPMNs are benign lesions that are more common in women and in individuals aged 60–69 years old. The MPMNs were typically round with smooth boundaries, had an average diameter of 5 mm, and were mostly distributed near the pleura. Some of the nodules appeared to have a cyst-like morphology. Pulmonary blood vessels could be found close to nodule edges. Most patients had a good prognosis, and the follow-up results were negative. By observing the pathological results, we explained the formation mechanism of CT signs and had a deeper understanding of the disease.

Acknowledgments

Funding: This work was funded by the Natural Science Foundation of China (Nos. 82102012 and 82102006).

Footnote

Reporting Checklist: The authors have completed the STROBE reporting checklist. Available at https://qims.amegroups.com/article/view/10.21037/qims-21-1250/rc

Conflicts of Interest: All authors have completed the ICMJE uniform disclosure form (available at https://qims.amegroups.com/article/view/10.21037/qims-21-1250/coif). The authors have no conflicts of interest to declare.

Ethical Statement: The authors are accountable for all aspects of the work in ensuring that questions related to the accuracy or integrity of any part of the work are

appropriately investigated and resolved. The study was conducted in accordance with the Declaration of Helsinki (as revised in 2013). The current study was approved by the Institutional Review Board of Nanjing Medical University. Written informed consent was provided by all participants before their participation in the study protocol.

References

1. Kuroki M, Nakata H, Masuda T, Hashiguchi N, Tamura S, Nabeshima K, Matsuzaki Y, Onitsuka T. Minute pulmonary meningothelial-like nodules: high-resolution computed tomography and pathologic correlations. J Thorac Imaging 2002;17:227-9.
2. Fadl SA, Pillappa R, Parker MS. Minute Pulmonary Meningothelial-like Nodules. Radiol Cardiothorac Imaging 2021;3:e210219.
3. Mizutani E, Tsuta K, Maeshima AM, Asamura H, Matsuno Y. Minute pulmonary meningothelial-like nodules: clinicopathologic analysis of 121 patients. Hum Pathol 2009;40:678-82.
4. Wen Z, Zhang Y, Fu F, Ma Z, Deng C, Ma X, Hu H, Sun Y, Chen H. Clinical, pathological and radiologic features of minute pulmonary meningothelial-like nodules. J Cancer Res Clin Oncol 2022;148:1473-9.
5. Korn D, Bensch K, Liebow AA, Castleman B. Multiple minute pulmonary tumors resembling chemodectomas. Am J Pathol 1960;37:641-72.
6. Kraushaar G, Ajlan AM, English JC, Müller NL. Minute pulmonary meningothelial-like nodules: a case of incidentally detected diffuse cystic micronodules on thin-section computed tomography. J Comput Assist Tomogr 2010;34:780-2.
7. Gaffey MJ, Mills SE, Askin FB. Minute pulmonary meningothelial-like nodules. A clinicopathologic study of so-called minute pulmonary chemodectoma. Am J Surg Pathol 1988;12:167-75.
8. Brambilla E, Travis WD, Colby TV, Corrin B, Shimosato Y. The new World Health Organization classification of lung tumours. Eur Respir J 2001;18:1059-68.
9. Huang EC, Zhang Y, Bishop JW, Gandour-Edwards RF, Afify AM. Diffuse pulmonary meningotheliomatosis: A diagnostically challenging entity on fine-needle aspiration cytology. Diagn Cytopathol 2015;43:727-30.
10. Churg AM, Warnock ML. So-called "minute pulmonary chemodectoma": a tumor not related to paragangliomas. Cancer 1976;37:1759-69.
11. Peng XX, Yan LX, Liu C, Wang SY, Li WF, Gao X, Wei XW, Zhou Q. Benign disease prone to be misdiagnosed as malignant pulmonary nodules: Minute meningothelioid nodules. Thorac Cancer 2019;10:1182-7.
12. Ohashi-Nakatani K, Shibuki Y, Fujima M, Watanabe R, Yoshida A, Yoshida H, Matsumoto Y, Tsuchida T, Watanabe SI, Motoi N. Primary pulmonary meningioma: A rare case report of aspiration cytological features and immunohistochemical assessment. Diagn Cytopathol 2019;47:330-3.
13. Lin D, Yu Y, Wang H, Fang Y, Yin J, Shen Y, Tan L. Radiological manifestations, histological features and surgical outcomes of pulmonary meningothelial proliferation: a case series and rethinking. Transl Lung Cancer Res 2020;9:1159-68.
14. Mukhopadhyay S, El-Zammar OA, Katzenstein AL. Pulmonary meningothelial-like nodules: new insights into a common but poorly understood entity. Am J Surg Pathol 2009;33:487-95.
15. Zhang Y, Wu J, Zhang T, Zhang Q, Chen YC. Minute pulmonary meningothelial-like nodules: rare lesions appearing as diffuse ground-glass nodules with cyst-like morphology. Quant Imaging Med Surg 2021;11:3355-9.

Cite this article as: Zhang Y, Wu J, Zhao Y, Zhang T, Xu H, Chen YC. Minute pulmonary meningothelial-like nodules: associations between computed tomography and pathology features. Quant Imaging Med Surg 2023;13(1):462-470. doi: 10.21037/qims-21-1250

